

^{79}Br nuclear-quadrupole-resonance line shape and Raman-induced spin-lattice relaxation in the incommensurate phase of $\beta\text{-ThBr}_4$

Songhua Chen and David C. Ailion

Department of Physics, University of Utah, Salt Lake City, Utah 84112

(Received 13 March 1989)

We performed ^{79}Br nuclear-quadrupole-resonance (NQR) line-shape and spin-lattice relaxation time measurements in the incommensurate (I) system $\beta\text{-ThBr}_4$ over the temperature range 293–2.5 K. In addition, we extended the theory of the effects of Raman processes on amplitudon and phason spin-lattice relaxation in incommensurate systems by obtaining general expressions for the spectral densities and phason gap Δ_ϕ that are valid at all temperatures in the I phase. By measuring T_1 selectively for the different parts of the broadened NQR line in $\beta\text{-ThBr}_4$, we separately obtained the phason and amplitudon contributions, $T_{1\phi}$ and T_{1A} , respectively. A comparison between theory and the experimental data shows excellent agreement and demonstrates that spin-lattice relaxation in $\beta\text{-ThBr}_4$ is dominated by Raman processes. The phason gap Δ_ϕ was determined to be 0.072 ± 0.020 THz.

I. INTRODUCTION

In recent years considerable interest has developed in studying incommensurate (I) systems. Many techniques [neutron diffraction,¹ light-scattering² and infrared³ spectroscopy, nuclear magnetic resonance (NMR),^{4,5} electron paramagnetic resonance (EPR) (Ref. 4 and 5), and nuclear quadrupole resonance (NQR) (Refs. 4 and 5)] have been successfully employed.

The incommensurate modulation wave is characterized by two excitation modes: (1) amplitudons, describing fluctuations in the amplitude of the wave, and (2) phasons, describing fluctuations in its phase. Even though amplitudon excitations are characterized by a nonzero energy at zero-reduced wave vector ($k=0$), phasons should be gapless since they represent sliding of the modulation wave.⁶ However, in actual systems phasons are not usually gapless, but are characterized by an energy gap believed to arise from pinning of the modulation wave by imperfections.⁴ Even though scattering techniques (neutron diffraction, Raman scattering) have been widely used in determining the amplitudon gap Δ_A , they are less effective in phason gap Δ_ϕ determination, because they have difficulty in observing frequencies that are smaller than the damping coefficient Γ .

In contrast, NMR, NQR, and EPR have been particularly useful in studying both the amplitudon and phason properties of I systems. The usefulness of NQR, in particular, is due to the fact that the I modulation wave directly affects the electric-field-gradient (EFG) tensor through the nuclear displacements. The static parts of the EFG tensor are responsible for line broadening while the fluctuating parts of the EFG induce spin-lattice relaxation. By exciting selectively different parts of the NQR line and measuring the corresponding spin-lattice relaxation times T_1 , the phason and amplitudon contributions to the spin-lattice relaxation rate^{4,5,7} can be determined separately.

At the present time, the A_2BX_4 systems (e.g., Rb_2ZnCl_4 , Rb_2ZnBr_4 , etc.) have been intensely studied with magnetic resonance techniques. Both NQR and NMR (Refs. 8 and 9) have recently been employed to determine separately the amplitudon and phason contributions to the spin-lattice relaxation as well as the phason gap. To the best of our knowledge, both the phason and amplitudon relaxation properties are dominated by direct phonon processes in the I systems studied by magnetic resonance up to now. In this paper we report the first magnetic resonance observations of amplitudon and phason relaxation by Raman processes in an incommensurate phase ($\beta\text{-ThBr}_4$).

The paraelectric-incommensurate phase transition at $T_I=95$ K in $\beta\text{-ThBr}_4$ was first observed independently by NQR (Ref. 10) and optical spectroscopy.¹¹ The incommensurate modulation is characterized by a displacement of the bromide ions, while the thorium ions remain at their high-temperature paraelectric-phase lattice sites.¹² As a result, an NQR study of bromide nuclei allows direct observation of the incommensurate modulation in $\beta\text{-ThBr}_4$.

In this paper, we report pure NQR line shape (including thermal fluctuation effects) and T_1 measurements of ^{79}Br in $\beta\text{-ThBr}_4$ powder in the I phase over the temperature range 95 K down to 2.5 K. Also, we extended the theory of the effects of Raman processes on the spin-lattice relaxation by obtaining general expressions for the phason gap Δ_ϕ and for the spectral densities valid for all temperatures in the I phase.

II. EXPERIMENTAL DETAILS

The powder sample used in the experiments was obtained from Anderson Physics Laboratory, Urbana, Illinois. The nominal purity is 99.9% and it is reported to be free of oxides and oxyhalides (<700 ppm H_2O and OH^-), as measured by the coulometric Karl Fischer titra-

tion method). The powder sample was sealed in a quartz ampoule in an inert atmosphere, and was not opened after shipment to our lab, thereby guaranteeing no moisture contamination. Because of strong quadrupolar broadening we used the Hahn echo¹³ sequence in which we selectively excited only a small portion of the NQR line using rf pulses of relatively long duration.

Low temperatures were obtained by the helium flow method. The temperature controller (Lake-Shore) uses one sensor to control heating of the flowing helium and another sensor to read out the temperature near the sample. The temperature variation was typically $\lesssim 0.10$ K, during each measurement. Temperatures between 2.5 and 4 K were achieved by pumping on the liquid helium in the sample spaces.

III. LINE SHAPE MEASUREMENTS

In general, NMR or NQR line shapes of *I* systems are quasicontinuous in nature because the incommensurate modulation disturbs the translational lattice periodicity resulting in a large number of nonequivalent individual nuclear displacements. This essentially infinite number of nonequivalent nuclei significantly broadens the NQR lines.

Blinic^{4,5} and co-workers calculated the resonance line shape for two models: local and nonlocal. The former states that the NQR frequency $\nu(x_i)$ of a given nucleus depends only on the displacement of this *i*th nucleus. In one-dimensional (1D) modulated systems, the relation between ν and the displacement yields

$$\begin{aligned} \nu(x) = & \nu_0 + \nu_1 \cos[\varphi(x) + \varphi_0] \\ & + \nu_2 \cos^2[\varphi(x) + \varphi_0] + \dots, \end{aligned} \quad (1)$$

where ν_j is proportional to the *j*th power of the amplitude of the modulation wave. In the more general nonlocal treatment, effects due to the displacements of all the nuclei are included. As a result, nonlocal effects will give rise to different phase angles for the different terms in the expression for the NQR frequency:

$$\begin{aligned} \nu(x) = & \nu_0 + \nu_1 \cos[\varphi(x) + \varphi_1] \\ & + \nu'_2 + \nu_2 \cos^2[\varphi(x) + \varphi_2] + \dots, \end{aligned} \quad (2)$$

where ν_0 corresponds to the high-temperature normal-phase NQR frequency. ν_1 is proportional to the linear term of the modulation wave amplitude [$\propto (T_I - T)^\beta$] and ν_2 (and ν'_2) are proportional to the quadratic terms.^{4,5} The critical exponent β is determined by several different experimental methods¹ to be $\beta \simeq 0.315$ in β -ThBr₄.

For β -ThBr₄, the bromide atoms are located in planes of symmetry, so that the linear term (as well as higher-order odd terms) in Eq. (1) or (2) are absent. Thus, Eq. (1) or (2) reduces to a quadratic expression

$$\nu(x) = \nu_0 + \nu_2 \cos^2 \varphi(x) + O(\nu_4) \quad (3)$$

in the local approximation, and

$$\nu(x) = \nu_0 + \nu'_2 + \nu_2 \cos^2 \varphi(x) + O(\nu_4) \quad (4)$$

for the nonlocal case. Obviously, if we can ignore the higher-order terms, ν'_2 will be the only term reflecting nonlocal effects. Hence, if most parts of the nonlocal EFG tensor are canceled out due to lattice symmetry, the only effect of the remaining nonlocal term is to shift the whole line by an extra temperature-dependent factor ν'_2 .

In the plane-wave approximation, where $\varphi(x)$ is linear in *x*, which is valid throughout part of the *I* phase except at temperatures very close to the incommensurate-commensurate (*I-C*) transition T_C , the observed NQR frequency distribution is given by⁵

$$f(\nu) = \frac{\text{const}}{[(\nu - \nu'_2 - \nu_0)(\nu_2 + \nu'_2 + \nu_0 - \nu)]^{1/2}} \quad (5)$$

for the nonlocal case. As a result, the NQR spectrum will exhibit two edge singularities, at

$$\nu_- = \nu_0 + \nu'_2$$

and (6)

$$\nu_+ = \nu_0 + \nu_2 + \nu'_2.$$

By comparing Eq. (6) to Eq. (4) we see that ν_- corresponds to $\cos \varphi(x) = 0$ and ν_+ to $\cos \varphi(x) = \pm 1$.

Figure 1 shows the NQR frequency measured as a function of temperature from 300 K down to 2.5 K. The splitting frequencies below $T_I \approx 95$ K in Fig. 1 are very close to those reported by Malek and co-workers,¹⁰ who also observed NQR splittings in the *I* phase down to about 65 K. The quantities ν_2 and ν'_2 can be obtained from the experimental values for ν_+ and ν_- since, from Eq. (6),

$$\nu_2 = \nu_+ - \nu_-$$

and (7)

$$\nu'_2 = \nu_- - \nu_0.$$

The paraelectric-phase NQR frequency ν_0 has linear temperature dependence with a negative slope of magnitude $d\nu_0/dT = 0.65$ kHz/K, as determined from the data above T_I in Fig. 1. Extrapolating this slope into the *I* phase, we can obtain "experimental" values for ν_2 and ν'_2 , using Eq. (7). Since ν_2 and ν'_2 are proportional to the square of the modulation wave amplitude, they are described by the expressions

$$\nu_2 = A (T_I - T)^{2\beta}$$

and (8)

$$\nu'_2 = B (T_I - T)^{2\beta}.$$

A fit to our experimental data, using $\beta = 0.315$, yields $A = (43.9 \pm 2.5)$ kHz/K^{2 β} and $B = (5.83 \pm 1.0)$ kHz/K^{2 β} . We thus see that B , which is a measure of the nonlocal effects, is only slightly more than 10% A . This relative unimportance of nonlocal effects can be understood qualitatively, since the *I* modulate wave displaces only the Br⁻ ions in β -ThBr₄, as discussed in Sec. I. The solid curves in Fig. 1 are obtained from Eq. (8) using the exper-

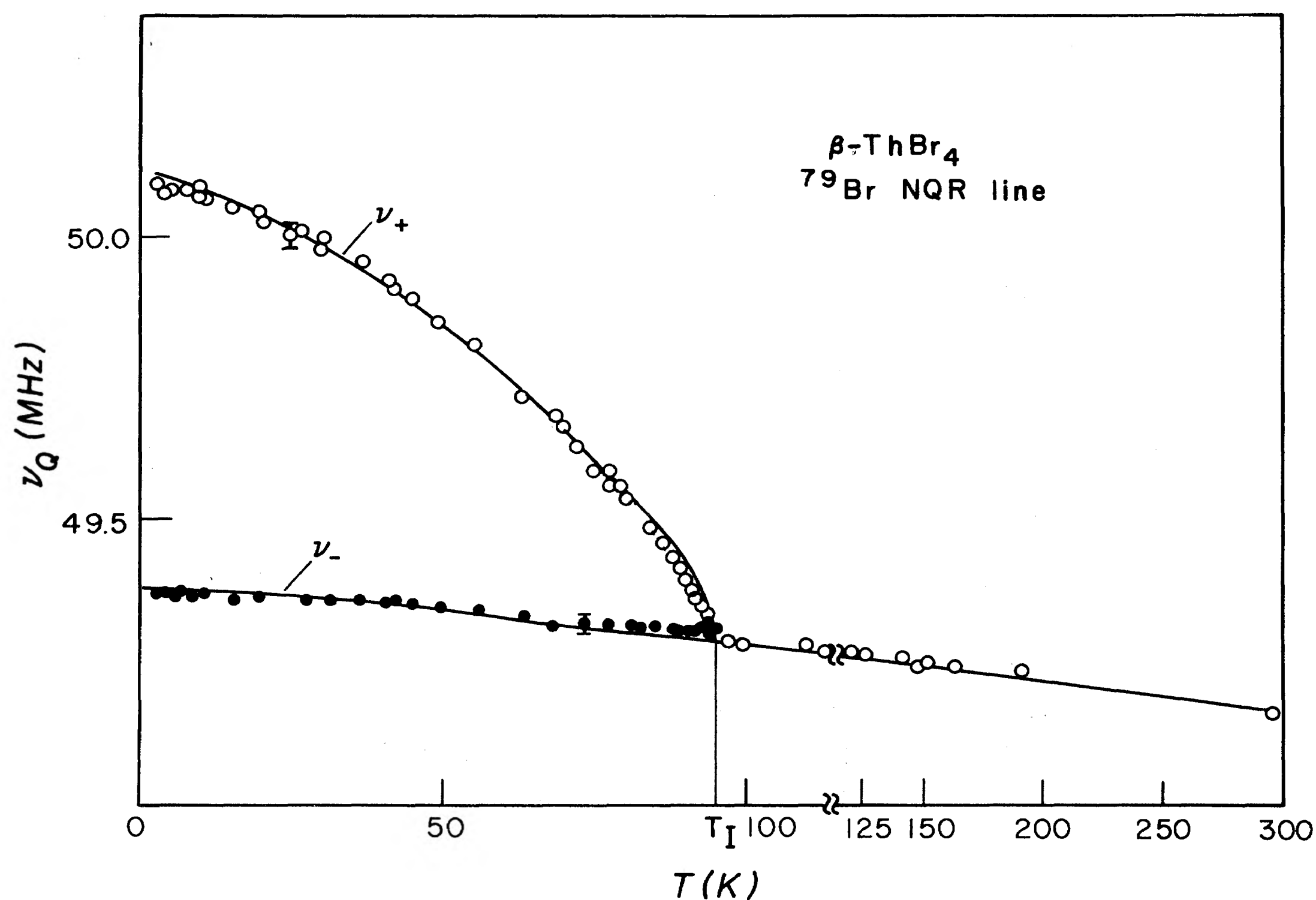


FIG. 1. Temperature dependence of NQR frequency ν_Q . Below T_I , the two sets of data are the frequencies of the singularities at $\nu_+ = \nu_0 + \nu_2 + \nu_2'$ and $\nu_- = \nu_0 + \nu_2'$.

imentally determined values for the fitting parameters A and B .

The excellent agreement between theory and experiment observed in temperature regions far from the vicinity of T_I is consistent with neutron scattering and other results¹⁴ showing that β is nearly a constant in the whole I phase. Furthermore, the line at 4.2 K is still a continuous inhomogeneous line with only two singularities (Fig. 2), characteristic of a typical I phase NQR frequency distribution.⁵ The absence of any discrete multisoliton lines indicates that we are not seeing any evidence of a nearby transition to a commensurate phase down to 2.5 K. The small deviation from the theoretical curve of the low-temperature data below 10 K may very well be due to a slight change in lattice parameter with decreasing temperature.

IV. THERMAL FLUCTUATIONS NEAR T_I

At temperatures immediately below the $P-I$ transition at $T_I = 95$ K, there is a small discrepancy between the measured singularity positions ν_+, ν_- and the theoretical expression [Eq. (6)], based on the classical Landau theory. Figure 3 shows an enlargement of the $T_I > T > T_I - 15$ K region. The solid line is the theoretical curve for $\nu_2 = 43.9(T_I - T)^{2\beta}$ and $\nu_2' = 5.83(T_I - T)^{2\beta}$ with $\beta = 0.315$. Qualitatively, we see motional narrowing due to rapid phase fluctuations¹⁵ of the modulation wave. Similar phenomena were also observed in Rb_2ZnBr_4 by NMR,¹⁶ Rb_2ZnCl_4 by NQR,¹⁷ and in Gd^{3+} -doped $\beta\text{-ThBr}_4$ by ESR.¹⁸

Below and near the $P-I$ transition temperature T_I , the phase of the modulation wave⁶ exhibits significant thermal fluctuations

$$\phi(x, t) = \phi(x) + \Delta\phi(x, t), \quad (9)$$

resulting in motional narrowing of the NQR line. At temperatures very close to T_I (say, within 1 K), phase

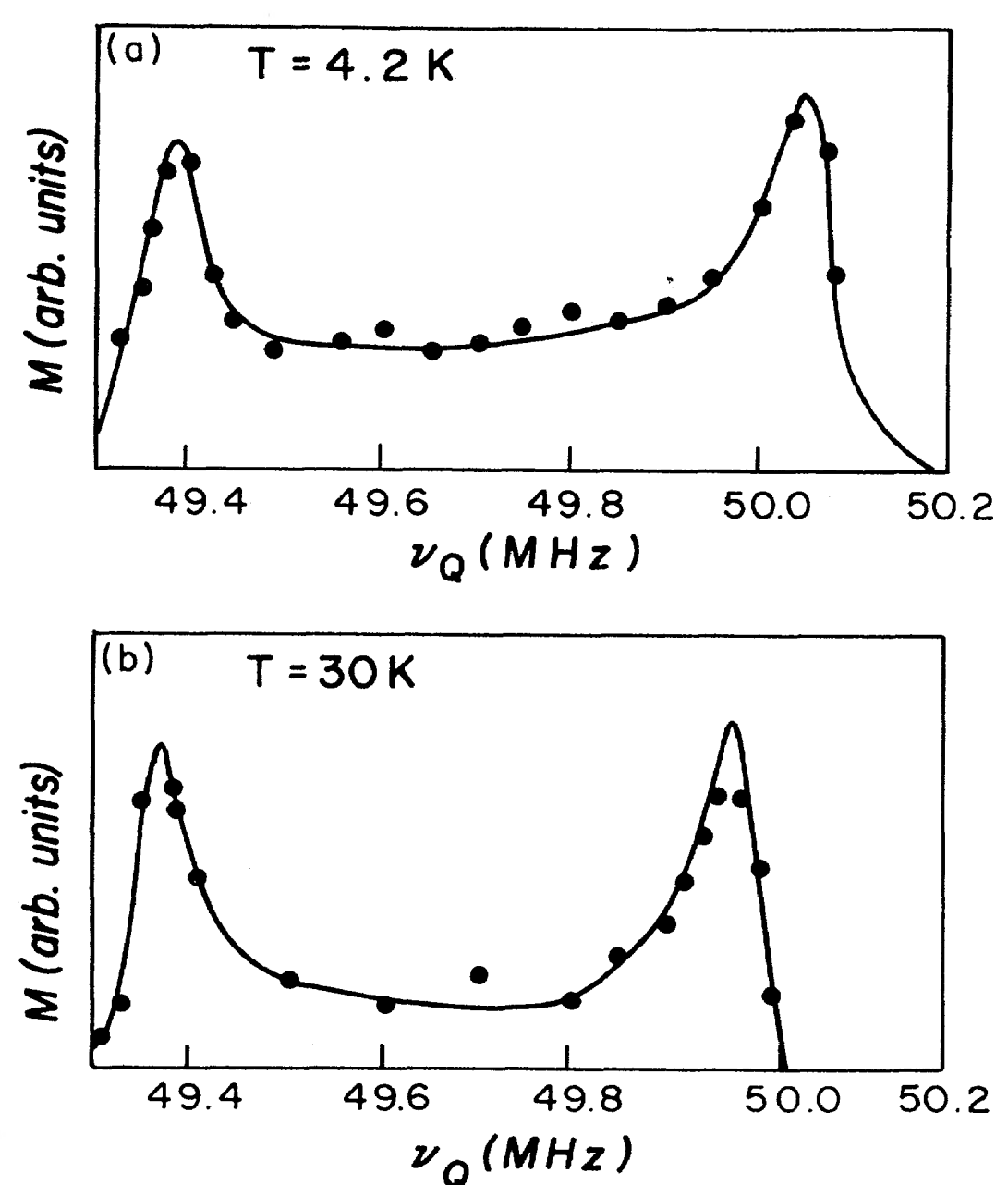


FIG. 2. NQR line shapes at (a) 4.2 K, (b) 30 K. Note that no multisoliton lines are observed.

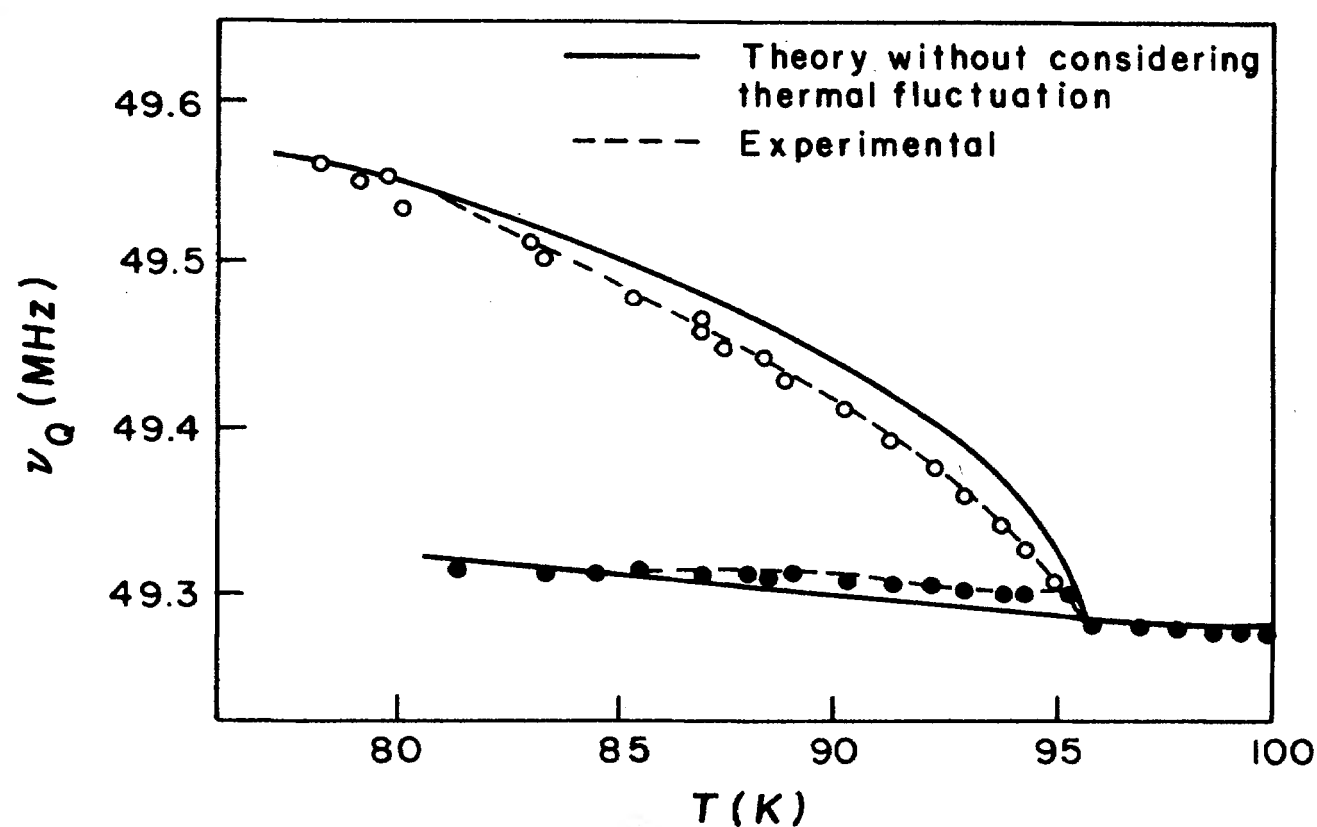


FIG. 3. Singularity splitting over the range $T_I - 15 < T < T_I$. The departure of the experimental results from the theoretical curve is due to motional narrowing arising from thermal phase fluctuations.

fluctuations will be rapid compared to the NQR time scale so that the motional averaging effect will result in a smoothing of the edge singularities, thus making it difficult to determine accurately the precise P - I transition temperature T_I . At lower temperatures, the edge singularities can be seen even though the linewidth may still be somewhat reduced by motional narrowing. In the quadratic approximation, Blinc and co-workers⁵ have shown that

$$\nu = \nu_0 + \frac{1}{2}[\nu_2 + \nu_2 e^{-2\sigma^2} \cos(2\phi)] + \nu'_2, \quad (10)$$

where $\sigma^2 = \overline{\Delta\phi^2}$ is a measure of the phase fluctuations. The singularities ν_{\pm} are then given by

$$\nu_{\pm} = \nu_0 + \frac{1}{2}\nu_2(1 \pm e^{-2\sigma^2}) + \nu'_2. \quad (11)$$

Decreasing the temperature causes $\sigma^2 \rightarrow 0$, in which case Eq. (11) reduces to Eq. (6).

The phase-fluctuation exponent σ^2 can be determined from a comparison of the differences between the experimental values for ν_+ and ν_- with the theoretical differences at each temperature in Fig. 3. From Eq. (11), we see that

$$\sigma^2 = -\frac{1}{2} \ln \frac{(\nu_+)_{\text{expt}} - (\nu_-)_{\text{expt}}}{(\nu_+)_{\text{theor}} - (\nu_-)_{\text{theor}}}, \quad (12)$$

where $(\nu_{\pm})_{\text{expt}}$ and $(\nu_{\pm})_{\text{theor}}$ represent experimental and theoretical values for ν_{\pm} . The denominator $(\nu_+)_{\text{theor}} - (\nu_-)_{\text{theor}}$ in Eq. (12) is ν_2 and is equal to the difference between the theoretical values (solid curves) in Fig. 3.

Figure 4 is a plot showing the temperature dependence of σ^2 just below T_I . We see that the thermal phase fluctuations are only significant within 5 K of T_I . At 10 K below T_I , the rms phase fluctuations are less than 10°, and have disappeared entirely below $T_I - 12$ K. These results are comparable to values for σ^2 reported in Rb_2ZnBr_4 by NMR (Ref. 16) and in Rb_2ZnCl_4 by NQR.¹⁷ It appears that the thermal fluctuation effect extends to

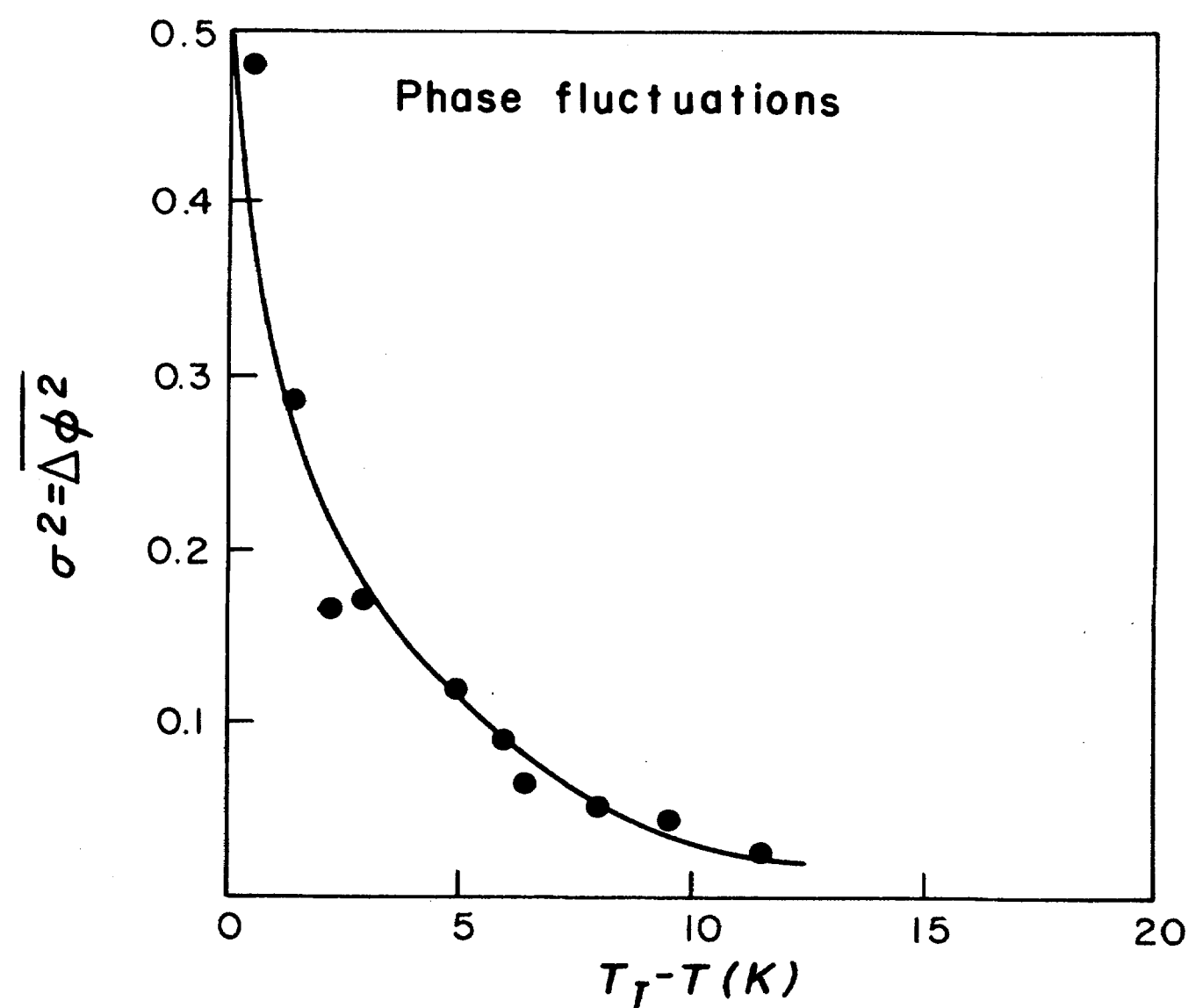


FIG. 4. Temperature dependence of the mean-square phase fluctuations $\sigma^2 = \langle \Delta\phi^2 \rangle$ in β - ThBr_4 .

slightly lower temperatures in our NQR measurements than were reported for EPR (Ref. 18) measurements in a Gd^{3+} -doped β - ThBr_4 crystal. This difference, which may result from possible pinning of the modulation wave by the dopant, reduces the amplitude of the phase fluctuations. Also, the ^{79}Br NQR technique may be more sensitive to slight changes in local environment due to small thermal fluctuations in the positions of the Br^- ions.

V. EFFECTS OF RAMAN PROCESSES ON T_{1A} AND $T_{1\phi}$

The general theory of the contributions of damped amplitudons and phasons to the NQR or quadrupolar perturbed NMR spin-lattice relaxation in incommensurate systems was developed by Blinc and co-workers.^{4,5,7} In contrast to the situation of translational periodic systems where T_I does not vary over the NQR line, amplitudons and phasons will contribute differently to different parts of the NQR spectrum in I systems, thereby allowing the independent determination of T_{1A} and $T_{1\phi}$.

Starting from the μ th component of the EFG tensor expanded in a Taylor series

$$\begin{aligned} T^{(\mu)}(t) &= T_0^{(\mu)} + \sum_i \left[\frac{\partial T^{(\mu)}}{\partial \mathbf{u}_i} \right]_0 \mathbf{u}_i(t) \\ &+ \frac{1}{2} \sum_{i,j} \left[\frac{\partial^2 T^{(\mu)}}{\partial \mathbf{u}_i \partial \mathbf{u}_j} \right]_0 \mathbf{u}_i(t) \otimes \mathbf{u}_j(t) + \dots \\ &= T_0^{(\mu)} + u T_{01}^{(\mu)} + u^2 T_{02}^{(\mu)} + \dots, \end{aligned} \quad (13)$$

where u is the magnitude of \mathbf{u}_i . The fluctuating part of the EFG tensor can be expressed⁴ as

$$\Delta T^{(\mu)}(t) = \sum_i \left[\left[\frac{\partial T^{(\mu)}}{\partial \mathbf{u}_i} \right]_0 + \sum_j \left[\frac{\partial^2 T^{(\mu)}}{\partial \mathbf{u}_i \partial \mathbf{u}_j} \right]_0 \mathbf{u}_j \right] \delta \mathbf{u}_i + \frac{1}{2} \sum_{i,j} \left[\frac{\partial^2 T^{(\mu)}}{\partial \mathbf{u}_i \partial \mathbf{u}_j} \right]_0 \delta \mathbf{u}_i \otimes \delta \mathbf{u}_j + \dots \quad (14)$$

The first term results in the direct process (absorption or emission of one phason or one amplitudon by the spin system) for relaxation and the second term results in the ordinary Raman process (inelastic scattering of two excitations, amplitudon or phason). From this expression, we see that the Raman process will be significant only if the linear term of the EFG tensor $(\partial T^{(\mu)}/\partial \mathbf{u}_i)_0 \approx 0$.

Furthermore, Raman processes should be important in spin-lattice relaxation only if there are considerable numbers of excitation pairs (versus single excitations) (Ref. 19) whose frequency differences correspond to the relatively low rf frequencies used in NMR and NQR. This situation should occur only when the density of excitations is peaked at frequencies much higher than the rf region, which, in turn, requires a small damping coefficient Γ (underdamped case). If, on the other hand, the excitation density is peaked at lower frequencies (near the NMR or NQR frequencies) which should occur when the damping coefficient is larger, direct processes should dominate the relaxation, as has been reported^{8,20,21} for most of the *I* systems (e.g., the A_2BX_4 systems) studied so far by NMR and NQR. However, even in these systems, the amplitudon modes are not strongly overdamped,²² suggesting that Raman processes may still be significant.

β -ThBr₄ has a relatively small damping coefficient¹⁴ ($\Gamma \approx 70$ GHz) compared with K₂SeO₄ for which $\Gamma \geq 210$ GHz.²² The β -ThBr₄ amplitudon gap Δ_A at 81 K was measured to be approximately 230 GHz by both Raman and neutron scattering.¹⁴ Therefore, it is quite obvious that the amplitudons are underdamped even at 81 K. There is insufficient experimental evidence in the literature to determine if there is a nonzero phason gap Δ_ϕ , which may be possibly induced by lattice defects or impurities. The phason dispersion curve reported at 81 K shows a maximum frequency $\omega_{\phi \max} \approx 400$ GHz. Since the damping coefficient Γ is smaller than these characteristic frequencies, there should be a large number of underdamped phason modes whose frequencies are much larger than the NQR frequency. As a result we would expect that both T_{1A} and $T_{1\phi}$ will be dominated by Raman processes in β -ThBr₄. Moreover, as we mentioned in Sec. III, the bromide atoms in β -ThBr₄ are located in planes of symmetry so that the part of the linear term in Eq. (14) involving $(\partial T/\partial \mathbf{u}_i)$ is absent, thereby reducing the contributions of direct processes to the spin-lattice relaxation.

If Raman processes are dominant in both phason- and amplitudon-induced relaxation in the local approximation, the spin-transition probability in the *I* phase will be given by⁴

$$\mathcal{W}^{(\mu)} = \frac{2}{3\pi} \left| \frac{e^2 Q}{h} T_{02}^{(\mu)} \right|^2 \left[\frac{kT}{\rho} \right]^2 \times [X^4 J_{AA} + (1-X^2)^2 J_{\phi\phi} + X^2(1-X^2)(J_{A\phi} + J_{\phi A})], \quad (15)$$

where $T_{02}^{(\mu)}$ is the EFG tensor component defined in Eq. (13), $X = \cos\varphi(x)$, ρ is the mass density, and $\mu = |\Delta m| = |\pm 1|, |\pm 2|, \dots$. The spectral densities for the amplitudon and phason contributions are represented by J_{AA} and $J_{\phi\phi}$, respectively. $J_{A\phi}$ and $J_{\phi A}$ are spectral densities for interactions involving one phason and one amplitudon. As we shall see in the present investigation T_{1A} and $T_{1\phi}$ will be determined without requiring a prior knowledge of $J_{A\phi}$ and $J_{\phi A}$. Since $T_1^{-1} = \mathcal{W}^{(1)} + \mathcal{W}^{(2)}$,

$$T_1^{-1} \propto (kT)^2 [X^4 J_{AA} + (1-X^2)^2 J_{\phi\phi} + X^2(1-X^2)(J_{A\phi} + J_{\phi A})]. \quad (16)$$

The amplitudon and phason contributions to the spin-lattice relaxation rate can be determined separately by selectively measuring T_1 in different parts of the line. At $X = \cos\varphi = 0, \nu = \nu_0$ in the local approximation [Eq. (3)] and

$$T_1^{-1} = \text{const } T^2 J_{\phi\phi}, \quad (17)$$

a pure phason contribution which we call $T_{1\phi}^{-1}$. At $X = \pm 1, \nu = \nu_0 + \nu_2$ and

$$T_1^{-1} = \text{const } T^2 J_{AA}, \quad (18)$$

a pure amplitudon contribution which we call T_{1A}^{-1} . At both $X = 0$ and ± 1 , the contributions from $J_{A\phi}$ and $J_{\phi A}$ vanish. A measurement of the temperature dependence of T_1^{-1} can thus be used to determine whether T_{1A} and $T_{1\phi}$ are dominated by Raman versus direct processes, since the contribution of the direct process to T_1^{-1} will be linear in temperature^{4,19} in contrast to the quadratic temperature dependence of Eqs. (15)–(18).

β -ThBr₄ is incommensurate over a wide temperature range, from $T_I = 95$ K down to the lowest temperature which we have investigated (2.5 K). Thus, it is very easy to distinguish a linear from a quadratic temperature dependence in the spin-lattice relaxation rate. Figure 5 shows the ⁷⁹Br spin-lattice relaxation times measured over the temperature range 293–2.5 K. In the vicinity of T_I we see a sharp dip, characteristic of soft-mode condensation. Below T_I , T_{1A} is measured at the higher-frequency edge singularity ν_+ (at $X = \pm 1$), whereas $T_{1\phi}$ is measured at the lower-frequency edge singularity ν_- (at $X = 0$).

In Fig. 6, we replot the *I* phase T_1 data as a log-log plot of T_{1A}^{-1} and $T_{1\phi}^{-1}$ versus T^2 . The fact that both curves have slopes equal to unity over most of the range indicates that both T_{1A}^{-1} and $T_{1\phi}^{-1}$ are dominated by Raman processes. Below approximately 10–15 K, the $T_{1\phi}^{-1}$ and T_{1A}^{-1} slopes becomes steeper than the T^2 dependence, as is typical for the low-temperature behavior of Raman processes. Near T_I , the amplitudon branch T_{1A}^{-1} increases rapidly, in contrast to $T_{1\phi}^{-1}$ which remains on the

T^2 curve, thereby indicating that J_{AA} is temperature dependent but $J_{\phi\phi}$ is not.

The spectral densities J_{AA} and $J_{\phi\phi}$ depend on the dispersion relations for amplitudons and phasons

$$\omega_A^2 = \Delta_A^2 + \kappa k^2 \quad (19)$$

and

$$\omega_\phi^2 = \Delta_\phi^2 + \kappa k^2, \quad (20)$$

where Δ_A and Δ_ϕ are the amplitudon and phason gaps, respectively. Figure 7 shows sketches of ω versus k obtained from Eqs. (19) and (20).

In the limit where the NQR frequency ν_Q is much less than the phason and amplitudon frequencies, Blinc⁴ showed that the spectral densities are

$$J_{AA} = \kappa^{-5/2} \Lambda (1 - 2\Delta_A / \Lambda \sqrt{\kappa}) \quad (21)$$

and

$$J_{\phi\phi} = \kappa^{-5/2} \Lambda (1 - 2\Delta_\phi / \Lambda \sqrt{\kappa}), \quad (22)$$

where Λ corresponds to the maximum value of the wave vector k . This treatment assumes the same value for

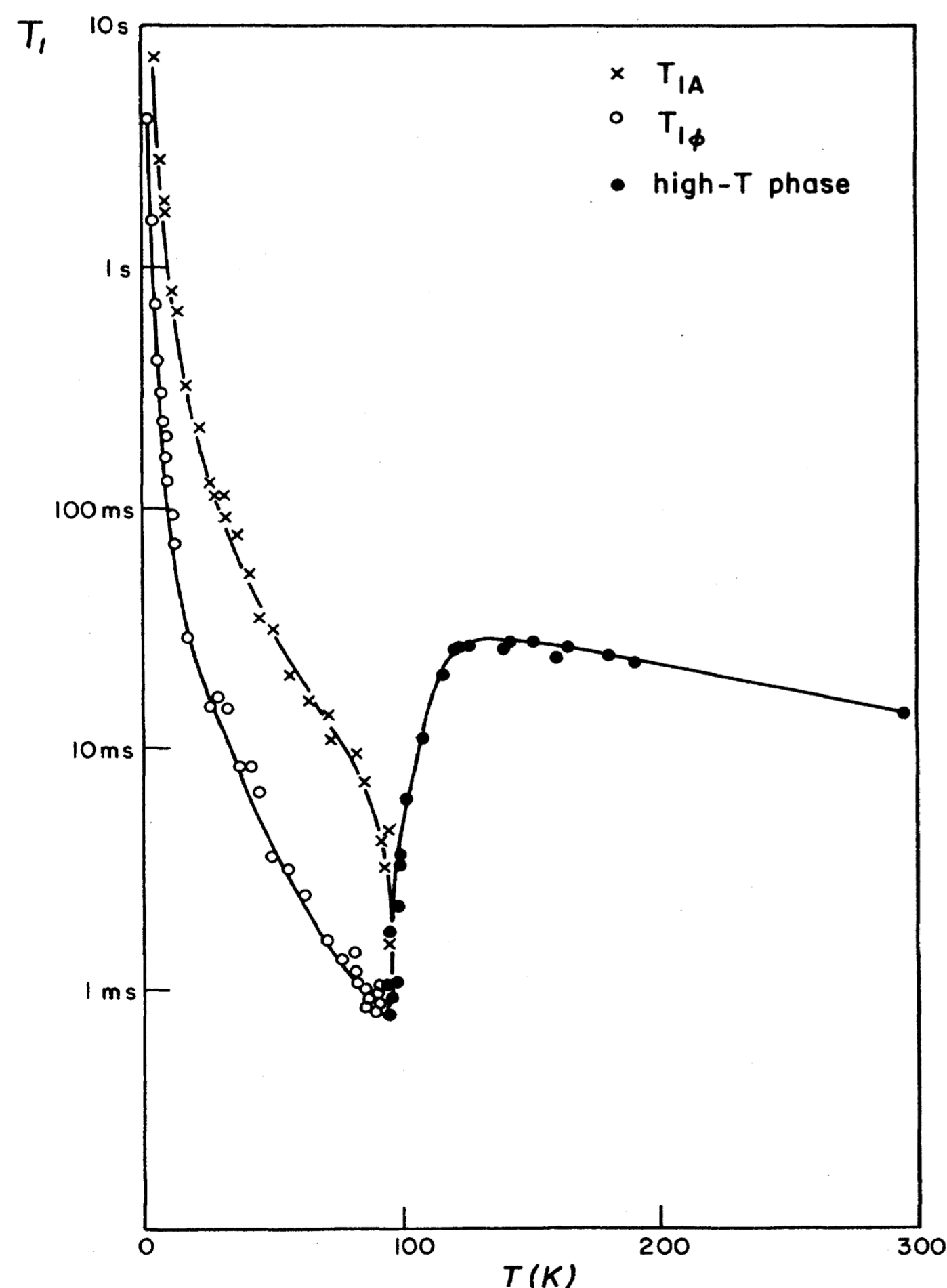


FIG. 5. Temperature dependence of the spin-lattice relaxation time T_1 . Below T_I , T_{1A} is measured at ν_+ and $T_{1\phi}$ is measured at ν_- .

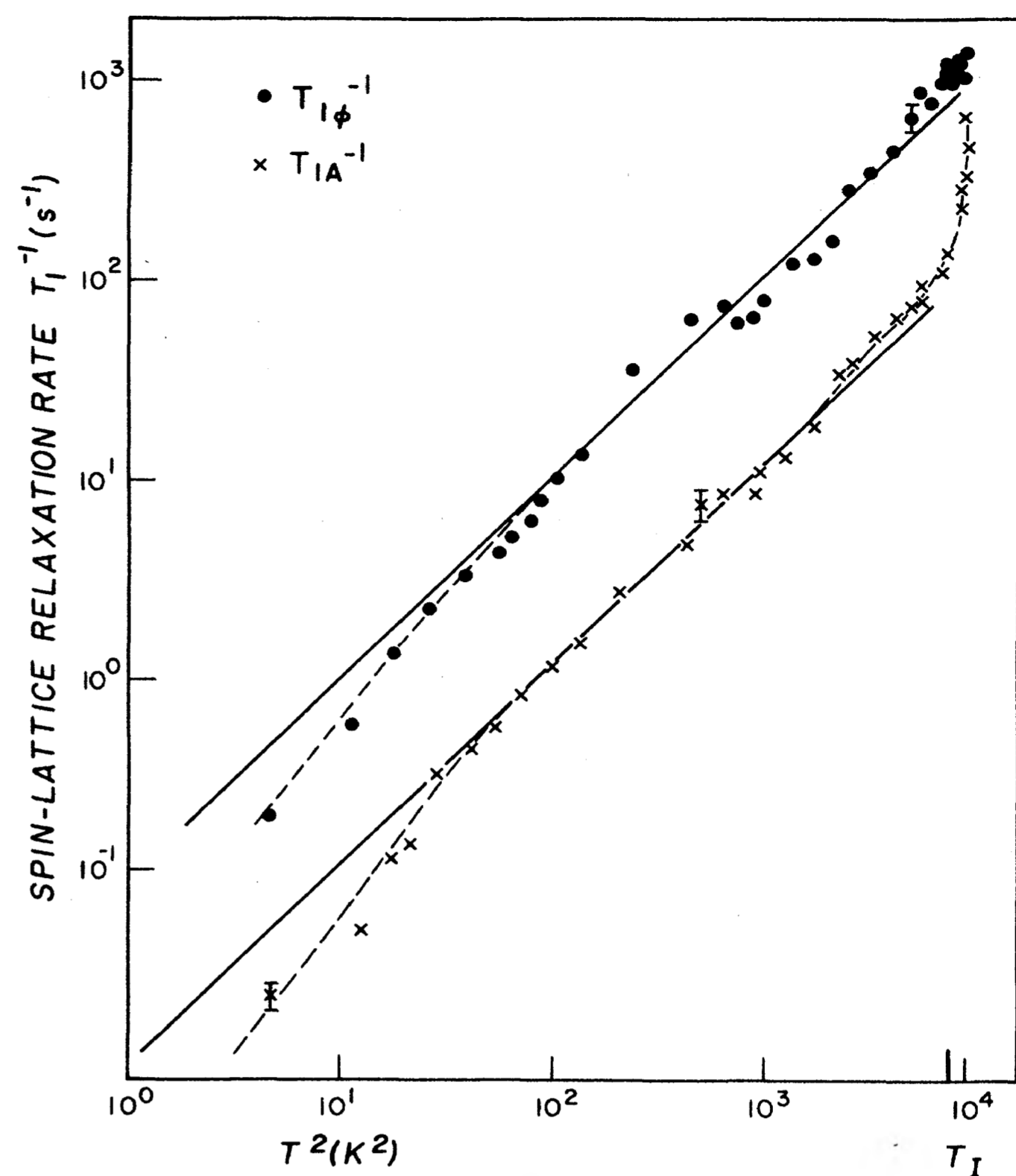


FIG. 6. Log-log plot of T_{1A}^{-1} and $T_{1\phi}^{-1}$ vs T^2 over the I phase. The solid lines at both branches have slopes of 1, indicating that Raman processes are dominant.

$\Lambda\sqrt{\kappa}$ for both phasons and amplitudons. Equations (21) and (22) are valid in the region very close to the transition temperature T_I . However, because $\Delta_A = \sqrt{2a(T_L - T)}$ is temperature dependent, $(2\Delta_A / \Lambda\sqrt{\kappa}) > 1$ and $J_{AA} < 1$ at temperatures far from T_I , causing Eq. (21) to no longer be valid. From published Δ_A data¹² at 81 K for β -ThBr₄, we can calculate

$$\sqrt{2a} = \Delta_A / \sqrt{T_I - 81 \text{ K}} = 235 / \sqrt{14} = 62.8 \text{ GHz/K}^{1/2}.$$

Using this value, we obtain at $T = 70$ K the value 314 GHz for Δ_A . Since $\Lambda\sqrt{\kappa}$ is temperature independent for

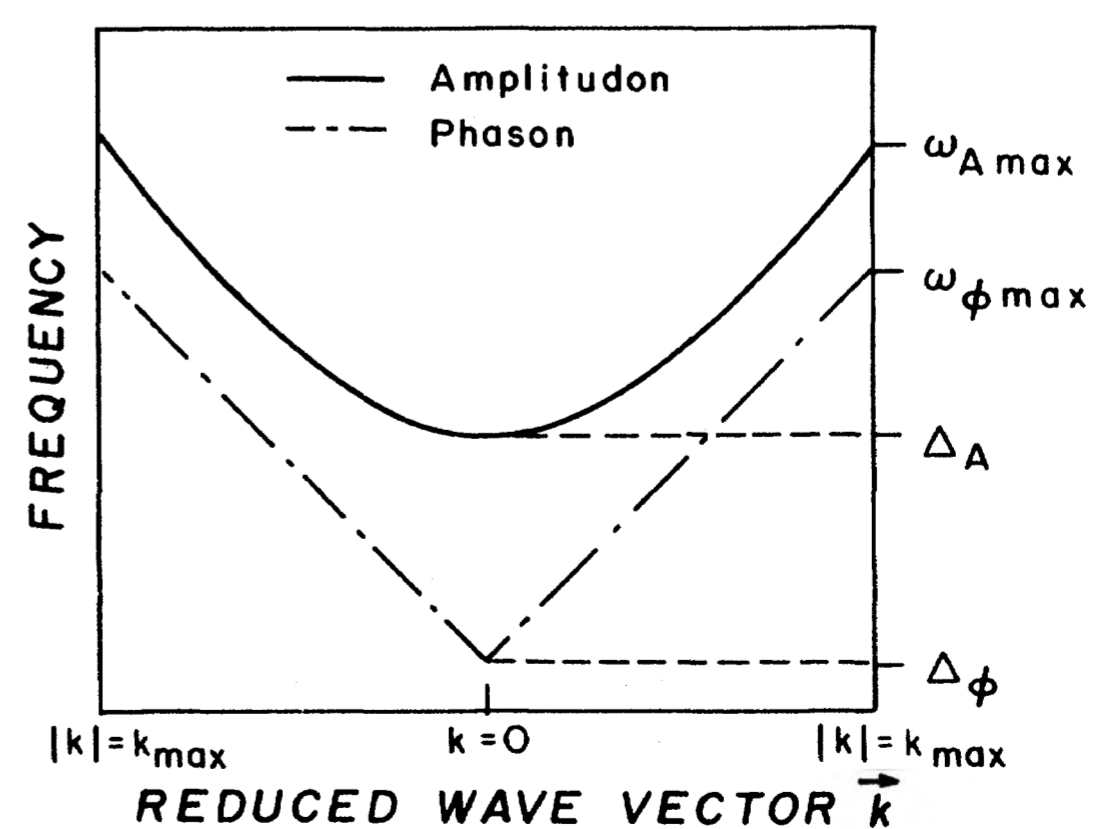


FIG. 7. Schematic diagram of typical I phase amplitudon and phason dispersion relations.

phasons, we can use the phason value $\Lambda\sqrt{\kappa} \approx 400$ GHz (Ref. 1) obtained at 81 K, in which case we see that $2\Delta_A/\Lambda\sqrt{\kappa} > 1$ and $J_{AA} < 1$. Thus, Eq. (21) is valid only at temperatures very close to T_I , for which $\Delta_A \ll \Lambda\sqrt{\kappa}$.

We extended Blinc and Zumer's treatment^{4,7} to obtain more general expressions for J_{AA} and $J_{\phi\phi}$, valid over most of the I phase, provided that the plane-wave approximation is valid. They expressed the spectral density $J_{\beta\beta'}$, where β and β' can be either A or ϕ , in terms of the excitation (phason or amplitudon) density ρ_{β} as

$$J_{\beta\beta'} = \frac{\pi^4}{V^2} \int \frac{\rho_{\beta}(\omega)\rho_{\beta'}(\omega+\omega_Q)d\omega}{\omega^2(\omega+\omega_Q)^2}. \quad (23)$$

Since we are interested only in J_{AA} and $J_{\phi\phi}$, we let $\beta=\beta'$ and obtain

$$J_{\beta\beta} = \frac{\pi^4}{V^2} \int \frac{\rho_{\beta}(\omega)\rho_{\beta}(\omega+\omega_Q)d\omega}{\omega^2(\omega+\omega_Q)^2}. \quad (24)$$

From the dispersion relations (19) and (20), we obtain

$$\frac{d\omega}{dk} = \frac{\kappa k}{\omega} = \sqrt{\kappa} [1 - (\Delta_{\beta}^2/\omega^2)]^{1/2}.$$

Since

$$\rho(\omega)d\omega = (V/4\pi^3)4\pi k^2 dk,$$

we get

$$\begin{aligned} \rho_{\beta}(\omega) &\approx \frac{V}{\pi^2} \kappa^{-3/2} \omega^2 [1 - (\Delta_{\beta}^2/\omega^2)]^{1/2}, \quad \omega > \Delta_{\beta}, \\ &= 0, \quad \omega \leq \Delta_{\beta}. \end{aligned} \quad (25)$$

There are two physically interesting limits for which we can evaluate $J_{\beta\beta}$.

(a) The gap $\Delta_{\beta} \gg \omega_Q$, in which case $\omega \gg \omega_Q$ and $\omega + \omega_Q \approx \omega$. We then get

$$\begin{aligned} J_{\beta\beta} &\approx \kappa^{-3} \int_{\Delta_{\beta}}^{\omega_{\beta\max}} \left[1 - \left(\frac{\Delta_{\beta}}{\omega} \right)^2 \right] d\omega \\ &= \kappa^{-3} \left[\omega_{\beta\max} - 2\Delta_{\beta} + \frac{\Delta_{\beta}^2}{\omega_{\beta\max}} \right] \\ &= \kappa^{-3} \frac{(\omega_{\beta\max} - \Delta_{\beta})^2}{\omega_{\beta\max}}. \end{aligned} \quad (26)$$

This result shows that $J_{\beta\beta}$ is always positive, as it should be.

(b) The gap $\Delta_{\beta} \ll \omega_Q$, so that $\rho_{\beta}(\omega) \approx (V/\pi^2)\kappa^{-3/2}\omega^2$ is the Debye result and we get

$$J_{\beta\beta} \approx \kappa^{-3} \int_0^{\omega_{\beta\max}} d\omega = \kappa^{-3} \omega_{\beta\max}. \quad (27)$$

Our result is more general than that of Blinc in two respects: (1) We kept the $\Delta_{\beta}^2/\omega_{\beta\max}$ term in Eq. (26), which is very small for T very close to T_I , but is not small for the amplitudon branch when T is far from T_I ; (2) we kept $\omega_{A\max}$ and $\omega_{\phi\max}$ distinct and did not assume them to be equal. From the dispersion relations Eqs. (19) and (20), we know that the maximum frequencies of the

two branches should be different and these differences become negligible only when Δ_{β} is very much less than $\omega_{\beta\max}$, which occurs in the amplitudon branch only for T very close to T_I . We thus see that Blinc's expressions for J_{AA} and $J_{\phi\phi}$ are approximations which are valid very close to T_I , whereas our modified expressions should be valid over most of the I phase.

VI. PHASON GAP Δ_{ϕ}

There exist relatively few examples of I systems in which a nonzero phason gap has been detected by direct experimental techniques (like neutron diffraction or optical spectroscopy), since phason excitations are usually overdamped ($\Gamma_{\phi} > \Delta_{\phi}$) near $k=0$. For β -ThBr₄, neutron scattering data are ambiguous^{1,14,23} about the existence of a nonzero phason gap, but suggest that the gap, if it exists in β -ThBr₄, should be at most 70 GHz.¹

Because of this difficulty in observing Δ_{ϕ} by the diffraction method, Blinc and co-workers studied several A_2BX_4 systems by spin-lattice relaxation measurements.^{4,5,16,20} All these studies assumed that both T_{1A} and $T_{1\phi}$ are direct processes, in which case,

$$\frac{\Delta_{\phi}}{\Delta_A} \approx \frac{J_{AA}}{J_{\phi\phi}} = \frac{T_{1A}^{-1}}{T_{1\phi}^{-1}}. \quad (28)$$

For Raman-dominated relaxation processes, we now derive a similar formula which can also be used to determine Δ_{ϕ} in those systems. Using Eq. (26) we get

$$\frac{T_{1A}^{-1}}{T_{1\phi}^{-1}} = \frac{J_{AA}}{J_{\phi\phi}} = \frac{\omega_{\phi\max}(\omega_{A\max} - \Delta_A)^2}{\omega_{A\max}(\omega_{\phi\max} - \Delta_{\phi})^2}, \quad (29)$$

assuming Δ_A and Δ_{ϕ} are much larger than ω_Q . The phason gap can then be calculated in terms of experimentally measurable quantities,

$$\Delta_{\phi} = \omega_{\phi\max} - \left[\left(\frac{\omega_{\phi\max}}{\omega_{A\max}} \right) \left(\frac{T_{1\phi}^{-1}}{T_{1A}^{-1}} \right) \right]^{1/2} (\omega_{A\max} - \Delta_A). \quad (30)$$

Theoretically, this formula is valid at any temperature in the I phase. However, it is preferable to perform measurements in the I phase at temperatures far below T_I for several reasons: (1) The dispersion relations [Eqs. (19) and (20)] are more valid at lower temperatures. A more general treatment¹⁴ results in a power series expansion

$$\begin{aligned} \omega^2 \begin{Bmatrix} A \\ \phi \end{Bmatrix} &= a |T_I - T| + G(k) \\ &\pm [a^2 |T_I - T|^2 + U^2(k)]^{1/2}, \end{aligned} \quad (31)$$

where $G(k) = \alpha_0 + \alpha_2 k^2 + \alpha_4 k^4 \dots$, $U(k) = \alpha_3 k^3 + \alpha_5 k^5 \dots$, and the + and - signs are associated with amplitudons and phasons, respectively. Only at lower temperatures will the terms involving $a |T_I - T|$ be sufficiently larger compared with $G(k)$ and $U(k)$ that the higher-order terms in the expansion can be neglected. In this case, Eq. (31) will reduce to Eqs. (19) and (20), keeping only terms quadratic in k . (2) Temperature measure-

ment inaccuracy can be a significant source of experimental error close to T_I , where T_{1A} is changing rapidly with temperature (Fig. 6). However, at lower temperatures, we see that the temperature dependence of the ratio $T_{1A}^{-1}/T_{1\phi}^{-1}$ is greatly reduced.

Evaluation of the phason gap by means of Eq. (30) requires knowledge of Δ_A , $\omega_{A\max}$, and $\omega_{\phi\max}$, which is easily obtained from other experimental measurements. In particular, neutron and Raman scattering measurements^{1,14} at 81 K give $\Delta_A \approx 0.23$ THz and $\omega_{\phi\max} \approx 0.4$ THz. By combining these results with our lower-temperature values for $T_{1\phi}$ and T_{1A} , we can use Eq. (30) to determine Δ_ϕ .

Since $\Delta_A(T) = \sqrt{2a(T_I - T)}$, we can express Δ_A at an arbitrary temperature in terms of its value at a particular temperature T_0 by

$$\Delta_A(T) = \Delta_A(T_0) [(T_I - T)/(T_I - T_0)]^{1/2}. \quad (32)$$

The maximum phason frequency $\omega_{\phi\max}$ and Δ_ϕ should be independent of temperature. The temperature dependence of $\omega_{A\max}$ can be expressed in terms of $\Delta_A(T)$ and $\omega_{\phi\max}$:

$$\begin{aligned} \omega_{A\max}(T) &= [\kappa k_{\max}^2 + \Delta_A^2(T)]^{1/2} \\ &\cong [\omega_{\phi\max}^2 + \Delta_A^2(T)]^{1/2}. \end{aligned} \quad (33)$$

Since $\Delta_\phi^2 \ll \omega_{\phi\max}^2$, the replacement of κk_{\max}^2 by $\omega_{\phi\max}^2$ is justified.

Using our measured relaxation times at $T = 50, 42,$ and 25 K, we obtained corresponding values for Δ_ϕ of 0.055, 0.088, and 0.087 THz, respectively. Our average value for Δ_ϕ (0.072 THz) is in good agreement with an upper limit for Δ_ϕ of 0.070 THz, estimated using other techniques.¹ The existence of a phason gap of this size strongly supports our contention that Raman (rather than direct) processes determine the relaxation, since

$$\Delta_\phi \gg \omega_Q (= 2\pi \times 50 \text{ MHz}).$$

VII. DETERMINATION OF T_1 VERSUS ν_Q OVER LINE SHAPE

It is important to consider the possibility that our spin-lattice relaxation is dominated by acoustic phonons (rather than amplitudons and phasons), which could also involve both direct and Raman processes. This possibility can be ruled out by a careful measurement of T_1 over the inhomogeneously broadened line shape since acoustic phonons should cause the same spin-lattice relaxation for all parts of the NQR line, whereas amplitudons and phasons will result in different values for T_1 for different parts of the line.⁴ Accordingly, we measured T_1 versus ν_Q at 4.2 and at 25 K over the whole line. Figure 8 shows a very strong dependence on ν_Q , thereby ruling out appreciable contributions from acoustic phonons.

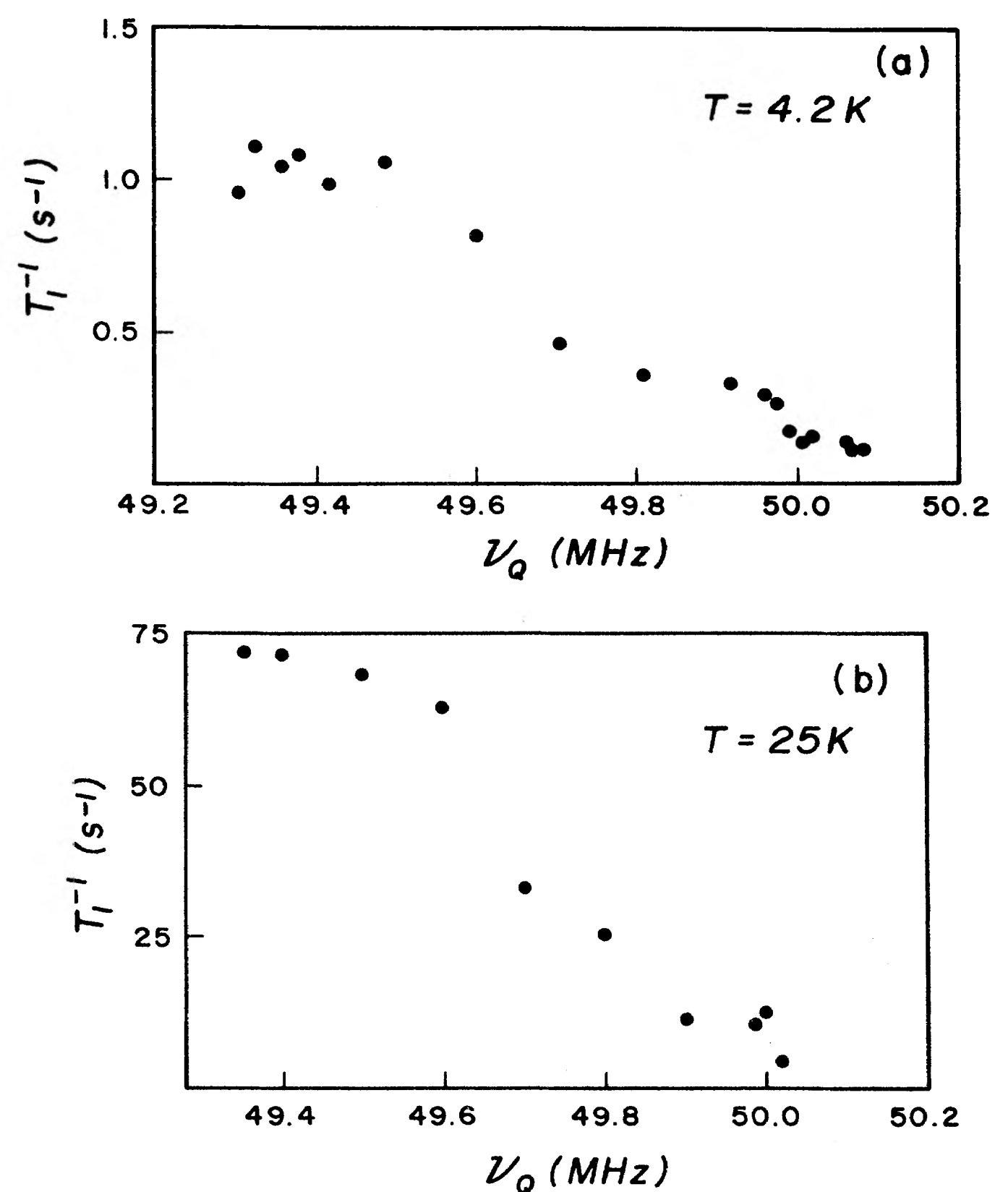


FIG. 8. T_1^{-1} vs ν_Q measured over whole NQR line (a) $T = 4.2$ K, (b) $T = 25$ K.

VIII. CONCLUSIONS

In this paper we extended the general theory, originally developed by Blinc,^{4,7} of the effects of Raman processes on amplitudon and phason spin-lattice relaxation in incommensurate systems. In particular we obtained general expressions for the phason and amplitudon contributions to the spectral densities that are valid at all temperatures in the I phase, not just near the transition temperature T_I . Also, we developed a general method for obtaining the phason gap Δ_ϕ in systems in which the spin-lattice relaxation is dominated by Raman processes.

We applied these techniques to ⁷⁹Br NQR in the incommensurate phase of β -ThBr₄ and found excellent agreement between our theoretical and experimental results, thereby demonstrating that spin-lattice relaxation in the incommensurate phase of this substance is indeed dominated by Raman processes. We measured the phason gap Δ_ϕ to be 0.072 ± 0.020 THz, in good agreement with estimates obtained from other experimental techniques.

We observed an incommensurate phase from $T_I (= 95$ K) down to our lowest temperatures (2.5 K). In particular, the absence of any sudden change in the line shape or spin-lattice relaxation time indicates the absence of any commensurate (C) phase over this temperature range. The absence of multisoliton effects and the constancy with temperature of $\beta = 0.315$ (Ref. 14) suggest that there

may not be a commensurate phase except possibly at significantly lower temperatures. However, if β -ThBr₄ is a type-II incommensurate system, multisoliton effects would not appear above the I - C transition temperature T_C ;^{24,25} hence, it is possible that a commensurate phase might exist slightly below our lowest temperature. More experiments at substantially lower temperatures are needed to resolve this question.

ACKNOWLEDGMENTS

The authors would like to express their thanks to Professor R. Blinc for reading this manuscript and to Dr. H. Kolem for scientific discussions and technical assistance with our cryogenic equipment. This research was supported in part by NATO under Grant No. RG 85/0081.

-
- ¹L. Bernard, R. Currat, P. Delamoye, C. M. E. Zeyen, S. Hubert, and R. de Kouchkovsky, *J. Phys. C* **16**, 433 (1983).
²H. Poulet and R. M. Pick, in *Incommensurate Phases in Dielectrics*, edited by R. Blinc and A. P. Levanyuk (North-Holland, New York, 1986), Vol. 1, Chap. 7.
³F. Gervais and P. Echegut, in *Incommensurate Phases in Dielectrics*, edited by R. Blinc and A. P. Levanyuk (North-Holland, New York, 1986), Vol. 1, Chap. 8.
⁴R. Blinc, *Phys. Rep.* **79**, 333 (1981).
⁵R. Blinc, R. Prelovsek, V. Rutar, J. Seliger, and S. Zumer, in *Incommensurate Phases in Dielectrics*, edited by R. Blinc and A. P. Levanyuk (North-Holland, New York, 1986), Vol. 1, Chap. 4.
⁶A. D. Bruce and R. A. Cowley, *J. Phys. C* **11**, 3609 (1978).
⁷S. Zumer and R. Blinc, *J. Phys. C* **14**, 465 (1981).
⁸S. Chen and D. C. Ailion, *Solid State Commun.* **69**, 1041 (1989).
⁹R. Blinc, P. Prelovsek, and R. Kind, *Phys. Rev. B* **27**, 47 (1983).
¹⁰K. Malek, C. A. Péneau, L. Guibé, P. Delamoye, and H. Hussonnois, *J. Mol. Struct.* **83**, 201 (1982).
¹¹S. Hubert, P. Delamoye, S. Lefrant M. Lepostollec, and M. Hussonnois, *J. Solid State Chem.* **36**, 36 (1981).
¹²C. P. Keijzers, G. Zwanenburg, J. M. Vervuurt, E. De Boer, and J. C. Krupa, *J. Phys. C* **21**, 659 (1988).
¹³E. L. Hahn, *Phys. Rev.* **80**, 580 (1950).
¹⁴R. Currat, L. Bernard, and P. Delamoye, in *Incommensurate Phases in Dielectrics*, edited by R. Blinc and A. P. Levanyuk (North-Holland, New York, 1986), Vol. 2, Chap. 15.
¹⁵R. Blinc, J. Seliger, and S. Zumer, *J. Phys. C* **18**, 2315 (1985).
¹⁶R. Blinc, D. C. Ailion, P. Prelovsek, and V. Rutar, *Phys. Rev. Lett.* **50**, 67 (1983).
¹⁷V. Rutar and F. Milia, *Ferroelectrics* **66**, 101 (1986).
¹⁸J. Emery, S. Hubert, and J. C. Fayat, *J. Phys. Lett.* **45**, L693 (1984).
¹⁹F. Borsa and A. Rigamonti, in *Magnetic Resonance of Phase Transitions*, edited by F. J. Owens, C. P. Poole, Jr., and H. A. Farach (Academic, New York, 1974), Chap. 3.
²⁰R. Blinc, D. C. Ailion, J. Dolinsek, and S. Zumer, *Phys. Rev. Lett.* **54**, 79 (1985).
²¹R. Blinc, V. Rutar, J. Seliger, S. Zumer, Th. Rasing, and I. P. Aleksandrova, *Solid State Commun.* **34**, 895 (1980).
²²M. Quilichini and R. Currat, *Solid State Commun.* **48**, 1011 (1983).
²³C. M. E. Zeyen, *Physica* **120B**, 283 (1983).
²⁴A. P. Levanyuk, in *Incommensurate Phases in Dielectrics*, edited by R. Blinc and A. P. Levanyuk (North-Holland, New York, 1986), Vol. 1, Chap. 1.
²⁵A. D. Bruce, R. A. Cowley, and A. F. Murray, *J. Phys. C* **11**, 3591 (1978).